Dyes and Pigments 94 (2012) 120–126

Contents lists available at SciVerse ScienceDirect

Dyes and Pigments

journal homepage: www.elsevier.com/locate/dyepig

A new stilbazolium salt with perfectly aligned chromophores for second-order nonlinear optics: 4-*N*,*N*-Dimethylamino-4′-*N*′-methyl-stilbazolium 3-carboxy-4-hydroxybenzenesulfonate

Jianhong Yin [a], Liang Li [a], Zhou Yang [a,*], Mojca Jazbinsek [b,*], Xutang Tao [c], Peter Günter [b], Huai Yang [a,*]

[a] *Department of Materials Physics and Chemistry, School of Materials Science and Engineering, University of Science and Technology Beijing, Beijing 100083, PR China*
[b] *Nonlinear Optics Laboratory, Institute of Quantum Electronics, ETH Zurich, CH-8093 Zurich, Switzerland*
[c] *State Key Laboratory of Crystal Material, Shandong University, Jinan 250100, PR China*

ARTICLE INFO

Article history:
Received 30 August 2011
Received in revised form
17 November 2011
Accepted 3 December 2011
Available online 13 December 2011

Keywords:
Nonlinear optical (NLO) materials
Aligned chromophores
Single crystals
Hydrogen bond
Organic dye
Kurtz powder test

ABSTRACT

A new organic nonlinear optical crystal 4-*N*,*N*-dimethylamino-4′-*N*′-methyl-stilbazolium 3-carboxy-4-hydroxybenzenesulfonate (DSCHS) has been developed with very promising properties for quadratic nonlinear optical applications. DSCHS single crystals with non-centrosymmetric structure have been obtained from aqueous methanol solution. X-ray crystallographic analysis revealed that the crystal structure of DSCHS is triclinic *P*1 with the chromophores aligned perfectly parallel, leading to the maximum possible order parameter $<\cos^3\theta> = 1$ in the crystalline state, which is optimal for electro-optics, THz-wave generation and field detection applications. Kurtz powder test has shown that DSCHS exhibits a very large second-order optical nonlinearity, with a 30 percent higher second-harmonic signal than the well-known organic nonlinear optical crystal 4-*N*,*N*-dimethylamino-4′-*N*′-methyl-stilbazolium tosylate (DAST).

1. Introduction

There is considerable interest in organic nonlinear optical (NLO) materials with large second-order optical nonlinearities. This is on the one hand because of the convenient and easy way in which their molecular structures, and hence their properties, can be tuned for various applications [1–3]. On the other hand, the main merits of organic materials compared with inorganic ones for second-order NLO applications such as THz generation, electric-field detection, electro-optic modulation and second-harmonic generation (SHG) applications are the large macroscopic second-order NLO susceptibilities ($\chi^{(2)}$), low dielectric dispersion and ultrafast response to external electric fields [4,5]. Organic NLO materials are based on NLO molecules (chromophores), which should be oriented in a non-centrosymmetric way in a macroscopic material system in order to exhibit macroscopic second-order NLO response. There are several different strategies resulting in macroscopic $\chi^{(2)}$ organic materials, including ferroelectric liquid crystals [6], self-assembled films [7], Langmuir–Blodgett films [8], poled polymer films [5,9], as well as single crystals [2,10]. Among them, polar organic crystals are of special interest, since large NLO effects can be achieved due to the high density of chromophores in crystals, as well as the most stable packing of chromophores in macroscopic materials, resulting in a superior photochemical and thermal stability as compared with softer materials such as the widely studied poled polymers [11]. Furthermore, organic NLO crystals can be also produced in a bulk form and are therefore not limited to thin-film applications [10–13]. This is particularly important for frequency conversion applications such as terahertz-wave generation, where large interaction lengths are required [14]. State-of-the-art organic NLO crystal DAST (4-*N*,*N*-dimethylamino-4′-*N*′-methyl-stilbazolium tosylate) and its derivative DSTMS (4-*N*,*N*-dimethylamino-4′-*N*′-methyl-stilbazolium 2,4,6-trimethylbenzenesulfonate) have been recently introduced in commercial THz sources [15], with high figures of merit and large frequency bandwidths compared to semiconductor alternatives like ZnTe or GaAs [16,17]. It is therefore interesting to develop organic materials with improved quadratic NLO susceptibility and therefore further increase the efficiency for applications.

Particularly challenging for the development of efficient organic crystalline $\chi^{(2)}$ materials is to simultaneously achieve good NLO properties and good physical properties for the growth of crystals

---

[*] Corresponding authors. Tel.: +86 10 62333759.
E-mail address: yangz@ustb.edu.cn (Z. Yang).

0143-7208/$ – see front matter Crown Copyright © 2011 Published by Elsevier Ltd. All rights reserved.
doi:10.1016/j.dyepig.2011.12.004

suitable for applications. The ways to design molecules with a high microscopic nonlinearity are now well understood, however, it is presently not possible to predict their packing into a crystalline lattice, which is extremely important for their macroscopic NLO response. The macroscopic response will basically depend on the number density of chromophores, non-centrosymmetric packing with a preferably high order parameter, and influence of the intermolecular interactions. Many methods [7–11] have been developed to design organic molecules leading to a relatively high probability for non-centrosymmetric arrangement in a bulk form. Out of these, the method of using Coulomb interactions of ionic chromophores to promote crystallization has been proved to be one of the most effective strategies [7]. For example, DAST (4-*N*,*N*-dimethylamino-4′-*N*′-methyl-stilbazolium tosylate), composed of the stilbazolium-chromophore cation and tosylate anion is one of the most well-known NLO materials, which is because of its large macroscopic NLO susceptibility $\chi^{(2)} = 580 \pm 30$ pm/V and the electro-optic figure of merit $n^3r = 455 \pm 80$ pm/V at 1.55 μm [18,19]. Nevertheless, theoretical calculations and recent progress have shown that it is still possible to improve the NLO properties and crystal-growth characteristics so that they will be superior to those of DAST. In previous studies, several DAST analogs with a modified counteranion were synthesized to achieve such an enhancement [20–24]. Research has shown that even very minor changes in the structures of counteranion have an important effect on the lattice stacking [22–27]. Well-designed counteranions can induce non-centrosymmetric structures having even higher NLO activity than DAST [22]. This provides nearly endless design possibilities, as we can achieve the combination of good NLO properties and desirable physical properties by adjusting the structure of both the anion and the cation.

It has been recently observed that beside Coulomb forces, important intermolecular interactions in DAST and its analogues present weak hydrogen bonds [25]. In this paper, we report the synthesis, crystal structure and NLO properties of a series of DAST derivatives with 3-carboxyl group on the counteranions. The counteranion functional groups have been chosen to promote hydrogen bonds in order to better understand their influence on packing and physical properties of stilbazolium salts. Among them, DSCHS (4-*N*,*N*-dimethylamino-4′-*N*′-methyl-stilbazolium 3-carboxy-4-hydroxybenzenesulfonate) shows very high non-resonant powder second-harmonic generation (SHG) efficiency of 30 percent higher than DAST, which is due to the perfectly parallel aligned chromophores.

2. Materials and methods

General Considerations. All reagents were purchased as high purity from Aldrich and used without further purification. ^{1}H-NMR spectra were recorded on a Brucker 400 MHz spectrometer on DMSO-d_6 solutions. Thermal analysis was conducted on Perkin–Elmer Pyris 6 DSC spectrometer at a heating rate of 10 °C/min.

DAST derivatives were synthesized via metathesization of 4-*N*,*N*-dimethylamino-4′-*N*′-methyl-stilbazolium iodide with the sodium salts of counteranions with 3-carboxyl group. The iodide salt was prepared from 4-picoline and iodomethane, and 4-(dimethylamino)benzaldehyde in the presence of piperidine as described in literature [1]. DAST derivatives were then recrystallized from methanol to get high purity materials for crystal growth.

4-*N*,*N*-dimethylamino-4′-*N*′-methyl-stilbazolium 3-carboxy-4-hydroxybenzenesulfonate (DSCHS): yield 75%; ^{1}H NMR (400 MHz, DMSO-d_6): $\delta = 8.68$(d, 2H, $J = 6.1$ Hz, C_5H_4N), 8.04(d, 3H, $C_5H_4N + C_7H_5O_6S$), 7.91(d, 1H, $J = 16.0$ Hz , C_2H_2), 7.68(d, 1H, $J = 8.5$ Hz, $C_7H_5O_6S$), 7.60(d, 2H, $J = 8.0$ Hz, C_6H_4), 7.18(d, 1H, $J = 16.1$ Hz , C_2H_2), 6.87(d, 1H, $J = 8.5$ Hz, $C_7H_5O_6S$), 6.79(d, 2H, $J = 8.1$ Hz, C_6H_4), 4.17(s, 3H, NMe), 3.02(s, 6H, NMe_2). Calcd for $C_{23}H_{24}N_2O_6S$: C, 60.51; H, 5.30; N, 6.14%. Found: C, 60.53; H, 5.29; N, 6.12%.

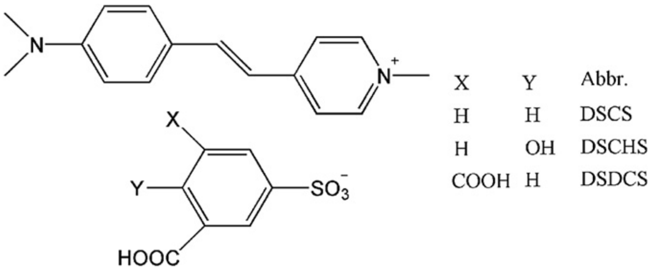

Fig. 1. Molecular diagram of DAST derivatives.

4-*N*,*N*-dimethylamino-4′-*N*′-methyl-stilbazolium 3-carboxybenzene-1-sulfonate (DSCS): yield 70%; ^{1}H NMR (400 MHz, DMSO-d_6): $\delta = 8.68$(d, 2H, $J = 6.8$ Hz, C_5H_4N), 8.19(s, 1H, $C_7H_5O_5S$), 8.04(d, 2H, $J = 6.8$ Hz, C_5H_4N), 7.92(m, 3H, $C_2H_2+C_7H_5O_5S$), 7.60(d, 2H, $J = 8.8$ Hz, C_6H_4), 7.46(t, 1H, $J = 15.3$ Hz, $C_7H_5O_5S$), 7.18(d, 1H, $J = 16.1$ Hz , C_2H_2), 6.79(d, 2H, $J = 8.8$ Hz, C_6H_4), 4.17(s, 3H, NMe), 3.02(s, 6H, NMe_2). Calcd for $C_{23}H_{24}N_2O_5S$: C, 62.71; H, 5.49; N, 6.36%. Found: C, 62.69; H, 5.27; N, 6.16%.

4-*N*,*N*-dimethylamino-4′-*N*′-methyl-stilbazolium 3,5-dicarboxybenzene-1-sulfonate (DSDCS): yield 72%; ^{1}H NMR (400 MHz, DMSO-d_6): $\delta = 8.68$(d, 2H, $J = 6.8$ Hz, C_5H_4N), 8.40(s, 1H, $C_8H_5O_7S$), 8.36(s, 2H, $C_8H_5O_7S$), 8.04(d, 2H, $J = 6.8$ Hz, C_5H_4N), 7.90(d, 1H, $J = 16.1$ Hz , C_2H_2), 7.58(d, 2H, $J = 8.8$ Hz, C_6H_4), 7.18(d, 1H, $J = 16.1$ Hz, C_2H_2), 6.79(d, 2H, $J = 8.8$ Hz, C_6H_4), 4.17(s, 3H, NMe), 3.02(s, 6H, NMe_2). Calcd for $C_{24}H_{24}N_2O_7S$: C, 59.49; H, 4.99; N, 5.78%. Found: C, 59.50; H, 5.06; N, 5.83%.

3. Results and discussion

3.1. Synthesis of DAST derivatives

DAST derivatives were successfully prepared by a three-step reaction approach; their structures were confirmed by ^{1}H NMR. The chemical structures of the three DAST derivatives are shown in Fig. 1. All of these new DAST derivatives possess 3-carboxyl group in the sulfonate counteranions. One of them, DSDCS possesses two carboxyl groups while DSCHS possesses one 4-hydroxyl group. These groups were chosen since they can lead to hydrogen bond formation, which could effectively influence the crystallographic packing of the stilbazolium-chromophore cation [25].

3.2. Physical properties

The melting point, UV absorption peak λ_{max} in solution, and powder SHG efficiency of the three DAST derivatives are listed in Table 1 compared to DAST. The melting points of all of the three DAST derivatives are quite higher than that of DAST and most of previously studied DAST derivatives [25–27]. These new

Table 1
Physical properties of the three DAST derivatives compared to DAST.

Compound	Melting point/°C	λ_{max}[a]/nm	Powder SHG[b]
DSCHS	>300	474	1.3
DSDCS	292 ± 1	474	0.1
DSCS	281 ± 1	474	0
DAST	256 ± 1	474	1

[a] In methanol solution at room temperature.

[b] 1907 nm fundamental radiation, compared with DAST, with an experimental error of less than 10%.

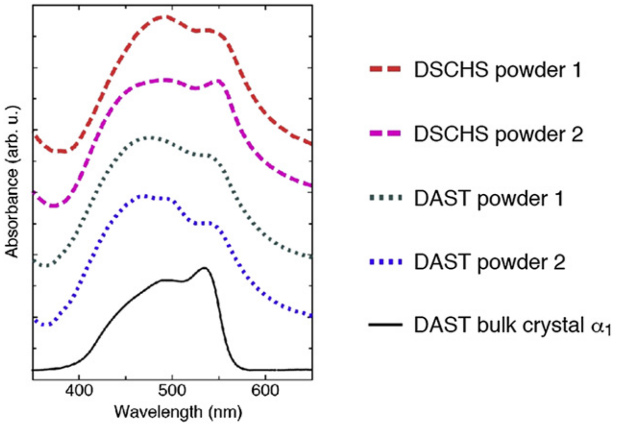

Fig. 2. Spectra of DSCHS and DAST powders compared to the absorption spectrum of DAST single crystals [28] along the polar axis. Differently prepared powders were measured to see the variation in spectra due to scattering.

compounds possess hydroxyl and carboxyl groups, which can form intermolecular hydrogen bonding, which is possibly one of the factors contributing to their high melting points. Hydrogen bonds in DSCHS crystal are discussed in more detail in Section 3.5. The wavelength of maximal absorption $\lambda_{max} = 474$ nm in methanol solution is the same for all compounds, which is because of the same NLO chromophore that contributes mainly to the charge transfer in these compounds. We also measured the spectra of the solid-state DSCHS in powder form in comparison with DAST, for that the absorption spectra in resonance have been previously fully characterized by more advanced methods using optically polished single crystals [28]. For this, we measured transmission spectra of thin layers of powders using a Perkin–Elmer Lambda 9 spectrometer. As shown in Fig. 2, both DSCHS and DAST show a red-shifted spectrum in solid state compared to solution, but their relative maxima are not considerably shifted, meaning that the molecular environment does not considerably change the electronic properties of the stilbazolium chromophore in the solid state for these two materials.

3.3. *Kurtz powder test*

The second-harmonic generation (SHG) efficiency of DSCHS was determined by using the Kurtz powder technique [29] in the same configuration as used in Ref. [22,25] An idler wave with a wavelength $\lambda = 1907$ nm from an optical parametrical amplifier pumped by an amplified Ti: sapphire femtosecond laser was used to screen the NLO activity of the new compound. DSCHS crystalline material was grinded and sieved to a particle size distribution of 63–90 μm, and then put into a 1.00 mm Hellma UV quartz sample cell to give a constant sample thickness. The scattered SHG signal at $\lambda = 954$ nm was detected by using appropriate filters. The SHG signals were calibrated with respect to equally prepared DAST samples. By this method we found that the SHG efficiencies of DSCHS and DSDCS are 1.3 and 0.1 times as that of DAST, respectively, while DSCS showed no signal pointing to the centrosymmetric final structure.

3.4. *Crystal growth*

DSCHS, whose counteranion possesses hydroxyl and carboxyl groups, was of most interest for crystal growth experiments because it showed a strong SHG activity 30% higher than DAST. However, DSCHS is not well soluble even in most polar solvents. After testing several common solvents and their combinations, we found that the solubility can be improved by using aqueous methanol solution with respect to both water and methanol alone. We compared solvent mixtures of methanol and water with 3:1, 2:1 and 1:1 proportion and found that DSCHS dissolved best using the last condition.

The slow cooling and slow evaporation methods are most suitable for crystal growth of the DSCHS. We performed crystal growth experiments by using the slow cooling method. The mixture of methanol and deionized water with 1:1 volume proportion was prepared as solvent. The DSCHS can be reasonably well-dissolved in the above mentioned solvent, although the solubility of 0.2 g/100 ml solvent at 45 °C is still much lower than the solubility 3.6 g/100 ml of DAST in methanol, which is the solvent most often employed for the crystal growth of DAST. We continued adding DSCHS to the solvent to prepare a saturated solution at 45 °C. After filtering the saturated solution by using 0.2 μm porosity Millipore filters at 45 °C, they were preheated to 45 °C to ensure that all ingredients were dissolved, then slowly cooled the solution from 45 °C to room temperature. The temperature was cooled down relatively fast at a rate of 2–3 °C per day without further optimization. It was found that red color DSCHS crystals start to nucleate and continue to grow in a plate-like shape preferentially along all edges in all directions. We filtered the solution and dried the crystals when the growth had stopped at room temperature.

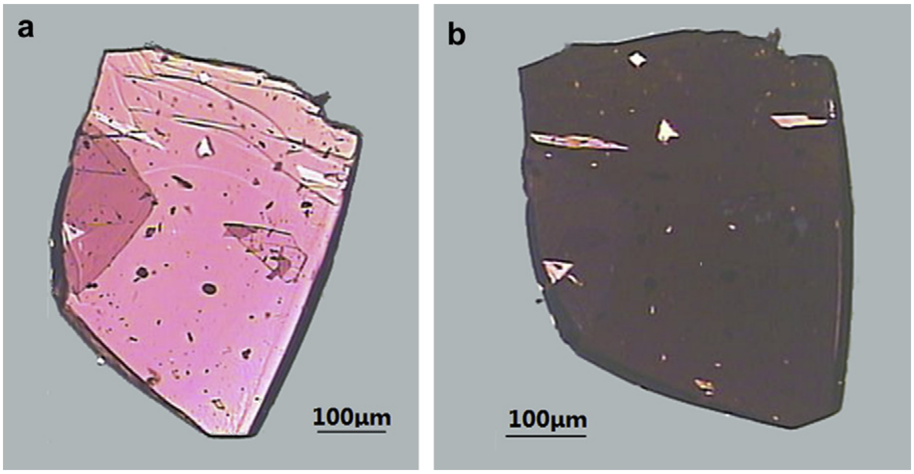

Fig. 3. Crystal of DSCHS between crossed polarizers in a microscope at the position of the maximum transmission (a) and rotated by 45° from this position (b).

Table 2
Crystallographic data of DSCHS.

Sample	DSCHS
Formula	$C_{23}H_{24}N_2O_6S$
Formula weight	456.50
Crystal system	Triclinic
Space group	P1
Point group	1
a/Å	7.1334
b/Å	8.5394
c/Å	9.965
α (°)	67.77
β(°)	70.65
γ (°)	75.29
Z	1
V/Å^3	524.4
Tm (°C)	173

We selected a thin plate crystal and placed it between crossed polarizers in a microscope (Fig. 3). Rotating the crystal by 45° around the direction of light propagation from the orientation with the highest transmission turned it completely dark, which means that in this case the main axis of the optical indicatrix (or its projection to the plane of the crystal plate) was aligned parallel to the polarization of the transmitted light, and also indicates that the crystals are single crystalline [18–20,25].

3.5. X-Ray crystallographic study

We measured the crystallographic structure of DSCHS by X-ray analysis of single crystals. The data obtained is listed in Table 2. DSCHS crystals are triclinic and have a P1 space group (point group 1); its crystal-packing diagram as seen along the crystallographic axes is shown in Fig. 4. The structure of one ion-pair is shown in Fig. 5. The chromophore's non-centrosymmetric alignment is a prerequisite for second-order NLO effects. In DSCHS the planar stilbazolium chromophores are aligned perfectly parallel, which represents the ideal case for adding up the microscopic polarizabilities into a macroscopic effect, maximizing the diagonal electro-optic and NLO coefficients.

It has been reported that DAST absorbs moisture easily to form a hydrate polymorph with centrosymmetric structure thus without second-order NLO properties [20]. The same phenomena have also been found from some other DAST derivatives, for example, DSTMS [24–26]. This means that for these stilbazolium salts the crystals must be grown in a completely nonaqueous environment to avoid forming centrosymmetric structure. In contrary for DSCHS, single crystals with a non-centrosymmetric structure have been obtained from aqueous solvent. Moreover, X-ray crystallographic data show that no water molecules have been included into the crystal structure of DSCHS.

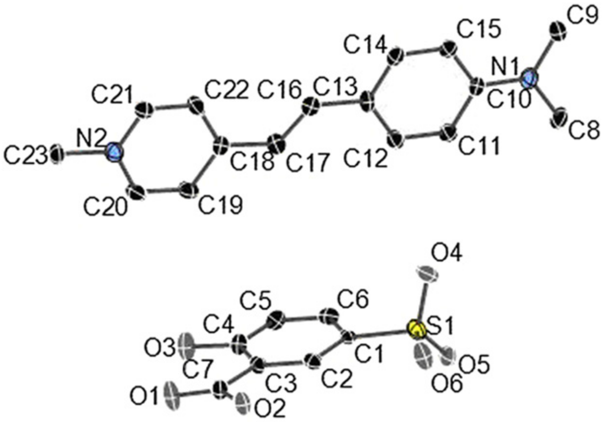

Fig. 5. Oak Ridge thermal ellipsoid program (ORTEP) representation of one ion-pair of DSCHS at 263 K (Vibrational ellipsoids are shown at the 30% probability level.)

Crystallographic data shows that beside the Coulomb interactions between the cation and anion parts, hydrogen bonds also play a role in crystal packing and chromophore orientation [25]. In DSCHS, the data shows that at least three kinds of hydrogen bonds have formed. One is the intermolecular hydrogen bond of O···H···O between the sulfonic oxygen atoms and carboxyl oxygen atoms with H···O distance of 1.754 Å; the other is intramolecular hydrogen bond of O···H···O between the hydrogen oxygen atoms and carboxyl oxygen atoms with H···O distance of 1.837 Å; the third are the weaker hydrogen bonds of C···H···O between the cation layers and the anion layers with H···O distances from 2.242 Å to 2.423 Å (Fig. 6). In DAST, strongest hydrogen bonds are weak hydrogen bonds between the cation and the anion layers with H···O distances of larger than 2.4 Å. Relatively strong hydrogen bonds may be one of the reason why DSCHS possesses a high melting point.

3.6. Discussion

We can estimate the expected powder test efficiency by considering the crystallographic packing of the chromophores and their density. In first approximation, we neglect any influence of the intermolecular interactions on the microscopic nonlinearity β of

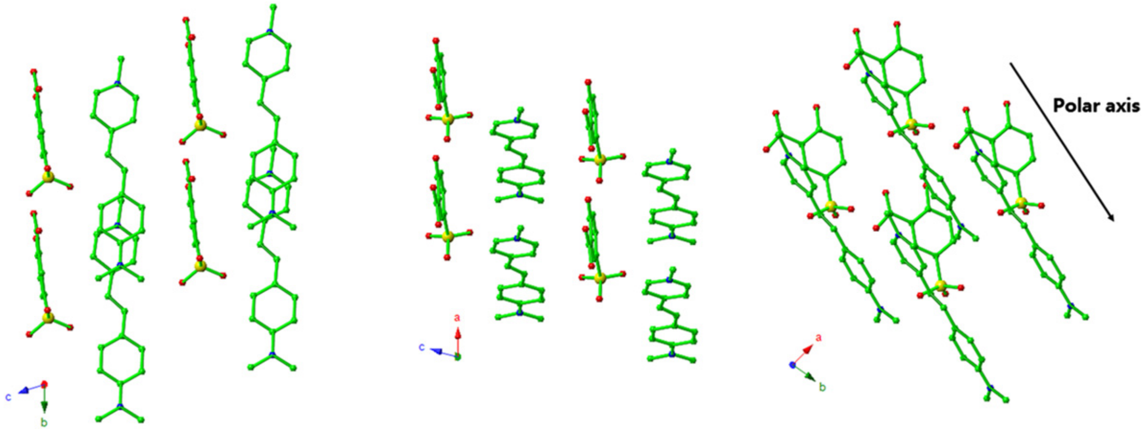

Fig. 4. Crystal-packing diagram: DSCHS with triclinic P1 symmetry viewed along the three crystallographic axes.

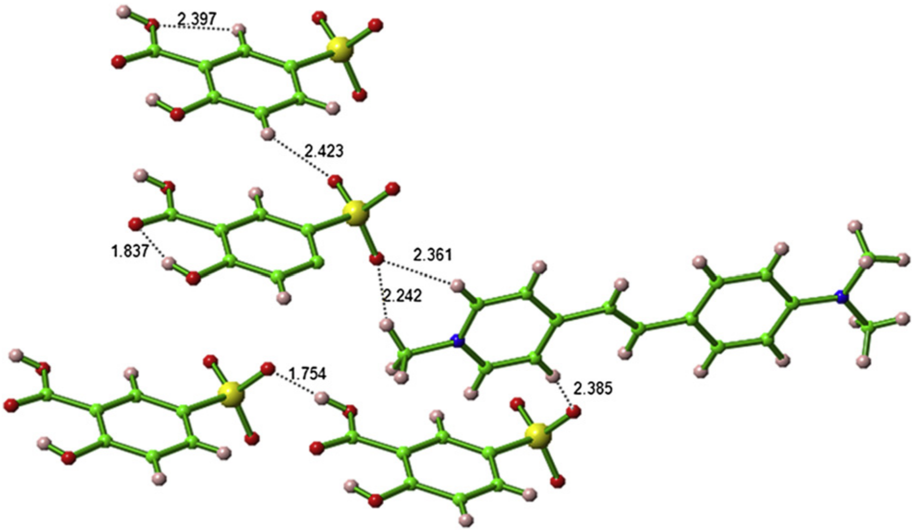

Fig. 6. The molecules in DSCHS are linked by Coulomb interactions between the ionic parts and by hydrogen bonds that are indicated by dotted lines.

the stilbazolium chromophore. This assumption is very reasonable considering the similar position of the absorption band observed in the powder spectrum (see Fig. 2). We also assume that the stilbazolium chromophore is essentially one-dimensional, with only one dominant component β of the first-hyperpolarizability tensor along the direction of the long axis of the chromophore, and neglect any contribution of the counteranion to the nonlinearity. In DAST, the four chromophores in the unit cell are aligned along the $3a + b$ and along the $3a - b$ crystallographic vectors, and therefore make an angle of about $\theta = 20^\circ$ with respect to the polar axis a. If we define the Cartesian system with its x axis parallel to a, y axis parallel to b, and z axis perpendicular to x and y, the effective hyperpolarizability of the crystalline system of DAST only contains the following components: $\beta_{111}^{\mathrm{eff}} = \beta\cos^3\theta = 0.83\beta$ and $\beta_{221}^{\mathrm{eff}} = \beta_{212}^{\mathrm{eff}} = \beta_{122}^{\mathrm{eff}} = \beta\cos\theta\sin^2\theta = 0.11\beta,$ according to the so-called oriented-gas model [24]. In case of DSCHS, $\theta = 0^\circ$, and only one effective hyperpolarizability component may be considered, $\beta_{111}^{\mathrm{eff}} = \beta$; in this case the x axis is chosen parallel to the chromophore, i.e. approximately along the $-a + 2b$ crystallographic vector that is also the polar axis of DSCHS (see Fig. 4c).

The powder test efficiency depends on the number density of the chromophores N and the squared effective β components, averaged over all possible orientations $\langle(\beta^{\mathrm{eff}})^2\rangle$ [29]. In case that only two effective components $\beta_{111}^{\mathrm{eff}}$ and $\beta_{221}^{\mathrm{eff}} = \beta_{212}^{\mathrm{eff}} = \beta_{122}^{\mathrm{eff}}$ are non-zero, $\langle(\beta^{\mathrm{eff}})^2\rangle$ can be expressed as [29] $\langle(\beta^{\mathrm{eff}})^2\rangle = \dfrac{1}{105}\ (19(\beta_{111}^{\mathrm{eff}})^2 + 13\beta_{111}^{\mathrm{eff}}\beta_{221}^{\mathrm{eff}} + 44(\beta_{221}^{\mathrm{eff}})^2)$, which gives $\langle(\beta^{\mathrm{eff}})^2\rangle_{\mathrm{DAST}} = 0.14\beta^2$ for DAST and $\langle(\beta^{\mathrm{eff}})^2\rangle_{\mathrm{DSCHS}} = 0.18\beta^2$. The number density of chromophores is in DSCHS very similar as in DAST, $N = 1.91 \times 10^{27}\ \mathrm{m}^{-3}$. Therefore we expect the non-resonant powder test efficiency of DSCHS, which is proportional to $N^2\langle(\beta^{\mathrm{eff}})^2\rangle$, to be about 30% larger than the one of DAST (1000 times that of urea) [3], if the molecular nonlinearity in the crystalline state is similar for both compounds. Since the powder size for this measurement was much larger than the coherence length of these compounds, which is in the order of magnitude of 1 μm, we also do not expect any substantial influence of the powder size. The experimental powder test efficiency perfectly agrees with our estimation, which confirms that the larger nonlinearity of DSCHS crystals compared to DAST is primarily due to the more optimal packing of the chromophores.

The perfectly parallel orientation of the chromophores is optimal to maximize the diagonal NLO susceptibility element. For phase-matched SHG applications in bulk materials, on the other hand, a high off-diagonal NLO susceptibility element is preferred, with the optimal angle θ of about 55° [30]. Such an orientation however reduces the maximal NLO susceptibility element by more than 60%; $\beta_{122,\max}^{\mathrm{eff}} \approx 0.38\beta$ at $\theta = 55^\circ$, while $\beta_{111,\max}^{\mathrm{eff}} \approx \beta$ at $\theta = 0^\circ$ [30]. Recently, most promising applications of organic NLO materials are within electro-optics, THz-wave generation and electric-field detection [9,13,16], for which a maximal possible NLO susceptibility element is optimal, as in the case of DSCHS.

In the last few years, there have been other DAST derivatives identified with isomorphous crystal structure as DSCHS, i.e. P1 space group with perfectly parallel chromophore orientation [25], so it is interesting to compare the observed powder test efficiency with these compounds. For all DAST derivatives crystallizing in space group P1, the theoretical spatial average $\langle(\beta^{\mathrm{eff}})^2\rangle = 0.18\beta^2$, the same as for DSCHS. The number density of the chromophores in these compounds is $N = 1.84 \times 10^{27}\ \mathrm{m}^{-3}$, $N = 1.79 \times 10^{27}\ \mathrm{m}^{-3}$, and $\mathrm{N} = 1.77 \times 10^{27}\ \mathrm{m}^{-3}$, for DSDMS, DSNS-1, and DSNS-2, respectively, see also Table 3. This gives the following theoretical powder test efficiencies relative to DAST: 1.2, 1.1, and 1.1 for DSDMS, DSNS-1, and DSNS-2, respectively, while the experimentally measured values were 0.7, 0.7 and 1.5 [25]. Since for all of these compounds the orientation of the chromophores is parallel, we expect that the relative experimental powder test results are rather accurate, since no other than diagonal components significantly contribute to the measured signal and therefore we also expect no contribution of eventual phase-matched SHG generation.

The large differences observed in experimental powder SHG tests are interesting because this indicates that intermolecular

Table 3
Comparison of DAST derivatives crystallizing in the space group *P*1.

Compound	DSCHS	DSDMS	DSNS-1	DSNS-2
N ($10^{27}\ \mathrm{m}^{-3}$)[a]	1.91	1.84	1.79	1.77
Theoretical Powder SHG[b]	1.3	1.2	1.1	1.1
Measured Powder SHG[c]	1.3	0.7	0.7	1.5

[a] The number density of the chromophores.

[b] Non-resonant conditions neglecting intermolecular interactions, relative to DAST.

[c] 1907 nm fundamental radiation, relative to DAST.

interactions play an important role in stilbazolium salts, and may enable to considerably enhance the molecular nonlinearity in the crystalline state, as also predicted for single-molecule molecular crystals [31]. For DAST, this has been suggested when comparing the measured macroscopic NLO susceptibility to the calculated one considering the molecular hyperpolarizability and using the oriented-gas model and the two-level model [32]. However, these models are greatly simplified in particular for strongly anisotropic dielectric systems such as stilbazolium salts. Therefore it is interesting to directly compare macroscopic crystals that contain the same NLO chromophore aligned in the same direction, but only having a different molecular environment of counteranion molecules, which is the case of crystals listed in Table 3. In Ref. [25], possible reasons for different measured values for the powder test efficiency of DSDMS, DSNS-1, and DSNS-2 were discussed. Since for DSNS-2 with the highest powder test efficiency the chromophore density is the lowest, one possible reason is that the larger chromophore separation will less reduce their molecular nonlinearity [25]. With our new compound DSCHS we see that this is not necessarily the case, since the density of the chromophores is in DSCHS considerably larger than in isomorphous DSDMS and DSNS-1 compounds, still it seems that the molecular nonlinearity is enhanced compared to these compounds. The influence of hydrogen bond formation of the stilbazolium chromophore with the surrounding counter ions was also investigated [25]. For DSDMS and DSNS-1 the strongest intermolecular hydrogen bonds involve the π-conjugated bridge of the chromophore, while for DSNS-2 they appear rather at the ends of the chromophore. Also in DSCHS the strongest hydrogen bonds involving the chromophore appear mostly at the ends of the molecule (see Fig. 6). This indicates that inducing strong hydrogen bonds at the ends of the stilbazolium chromophore may indeed be beneficial for their nonlinearity, since the powder test efficiency of DSNS-2 and DSCHS is almost twice as large as in DSDMS and DSNS-1, although in all of these compounds the chromophores are aligned perfectly parallel. The enhancement of the molecular nonlinearity has been also observed in non-ionic crystalline systems with hydrogen bonds as main interactions, in cases where head-to-tail hydrogen bonds were included [31,33,34].

The chromophores in DSCHS crystals are therefore packed perfectly parallel and their molecular environment does not diminish their nonlinearity as in some isomorphous crystals.

4. Conclusions

In summary, a series of new organic NLO stilbazolium salts with the same cation chromophore but different counteranion, which promotes hydrogen bonds, as compared to the well-known DAST, have been synthesized. Among them, DSCHS powder showed a very high second-order NLO activity, which is 30% higher than for DAST. Single crystals of DSCHS have been grown by a slow cooling technique. X-ray diffraction shows that the structure is triclinic and that the chromophores are aligned perfectly parallel with the highest possible order parameter $\cos^3\theta = 1$. This result confirms that the macroscopic second-order NLO properties of the organic NLO salts can be increased by selecting suitable counteranions to optimize the intermolecular interactions and chromophore packing. DSCHS crystals are therefore very interesting for applications where a high diagonal NLO coefficient is desired, such as electro-optics, THz-wave generation and electric-field detection.

Acknowledgments

This work was supported by the National Natural Science Foundation (grant no. 50803005), the Fundamental Research Funds for the Central Universities, the Scientific Research Foundation for the Returned Overseas Chinese Scholars, the National Natural Science Fund for Distinguished Young Scholar (Grant no. 51025313), and by the Swiss National Science Foundation.

References

[1] Ruiz B, Yang Z, Jazbinsek M, Gramlich V, Günter P. Synthesis and crystal structure of a new stilbazolium salt with large second-order optical nonlinearity. J Mater Chem 2006;16:2839–42.
[2] Bosshard C, Bösch M, Liakatas I, Jäger M, Günter P. In: Günter P, editor. Nonlinear optical effects and materials. Springer-Verlag; 2000.
[3] Marder SR, Perry JW, Schaefer WP. Synthesis of organic salts with large second-order optical nonlinearities. Science 1989;245:626–8.
[4] Coe BJ, Harris JA, Clays AK, Olbrechts G, Persoons A, Hupp JT, et al. Quadratic nonlinear optical properties of N-aryl stilbazolium dyes. Adv Funct Mater 2002;12:110–6.
[5] Dalton L. Nonlinear optical polymeric materials: from chromophore design to commercial applications. Adv Polym Sci 2002;158:1–86.
[6] Zhang YQ, Perdiguero JM, Baumeister U, Walker C, Etxebarria J, Prehm M, et al. Laterally Azo-bridged H-shaped ferroelectric dimesogens for second-order nonlinear optics: ferroelectricity and second harmonic generation. J Am Chem Soc 2009;131(51):18386–92.
[7] Frattarelli D, Schiavo M, Facchetti A, Ratner MA, Marks TJ. Self-assembly from the gas-phase: design and implementation of small-molecule chromophore precursors with large nonlinear optical responses. J Am Chem Soc 2009; 131(35):12595–612.
[8] Ashwell GJ. Langmuir–Blodgett films: molecular engineering of non-centrosymmetric structures for second-order nonlinear applications. J Mater Chem 1999;9:1991–2003.
[9] Dalton LR, Benight SJ, Johnson LE, Knorr DB, Kosilkin I, Eichinger BE, et al. Systematic nanoengineering of soft matter organic electro-optic materials. Chem Mater 2011;23:430–45.
[10] Jazbinsek M, Kwon OP, Bosshard C, Günter P. In: Nalwa SH, editor. Handbook of organic electronics and photonics. American Scientific Publishers; 2008 [chapter 1].
[11] Rezzonico D, Kwon SJ, Figi H, Kwon OP, Jazbinsek M, Günter P. Photochemical stability of nonlinear optical chromophores in polymeric and crystalline materials. J Chem Phys 2008;128:124713–8.
[12] Figi H, Mutter L, Hunziker C, Jazbinsek M, Gunter P, Coe BJ. Extremely large nonresonant second-order nonlinear optical response in crystals of the stilbazolium salt DAPSH. J Opt Soc Am B 2008;25(11):1786–93.
[13] Jazbinsek M, Mutter L, Günter P. Photonic applications with the organic nonlinear optical crystal DAST. IEEE J Sel Top Quantum Electron 2008;14(5):1298–311.
[14] Tonouchi M. Cutting-edge terahertz technology. Nature Photonics 2007;1: 97–105.
[15] http://www.rainbowphotonics.com/.
[16] Schneider A, Neis M, Stillhart M, Ruiz B, Khan RUA, Günter P. Generation of terahertz pulses through optical rectification in organic DAST crystals: theory and experiment. J Opt Soc Am B 2006;23(9):1822–35.
[17] Stillhart M, Schneider A, Günter P. Optical properties of 4-N,N-dimethylamino-4′-N′-methyl-stilbazolium 2,4,6-trimethylbenzenesulfonate crystals at terahertz frequencies. J Opt Soc Am B 2008;25(11):1914–9.
[18] Wong MS, Pan F, Bösch M, Spreiter R, Bosshard C, Günter P. Novel electro-optic molecular cocrystals with ideal chromophoric orientation and large second-order optical nonlinearities. J Opt Soc Am 1998;15:426–31.
[19] Okada S, Nogi K, Anwar Tsuji K, Duan XM, Oikawa H, Matsuda H, et al. Ethyl-substituted stilbazolium derivatives for second-order nonlinear optics. Jpn J Appl Phys 2003;42:668–71.
[20] Pan F, Wong MS, Bosshard C, Günter P. Crystal growth and characterization of the organic salt 4-N,N-dimethylamino-4′-N′-methyl-stilbazolium tosylate (dast). Adv Mater 1996;8:592–5.
[21] Yang Z, Wörle M, Mutter L, Jazbinsek M, Günter P. Synthesis, crystal structure and second-order nonlinear optical properties of new stilbazolium salts. Cryst Growth Des 2007;7:83–6.
[22] Yang Z, Aravazhi S, Schneider A, Seiler P, Jazbinsek M, Günter P. Synthesis and crystal growth of stilbazolium derivatives for second-order nonlinear optics. Adv Funct Mater 2005;15:1072–6.
[23] Marder SR, Perry JW, Schaefer WP. Organic salts with large second-order optical nonlinearities. Chem Mater 1994;6:1137–47.
[24] Yang Z, Mutter L, Stillhart M, Ruiz B, Aravazhi S, Stillhart M, et al. Large-size bulk and thin-film stilbazolium-salt single crystals for nonlinear optics and THz generation. Adv Func Mater 2007;17:2018–23.
[25] Yang Z, Ruiz B, Aravazhi S, Stillhart M, Jazbinsek M, Gramlich V, et al. Molecular engineering of stilbazolium derivatives for second-order nonlinear optics. Chem Mater 2007;19:3512–8.
[26] Coe BJ, Foxon SP, Harper EC, Harris JA, Helliwell M, Raftery J, et al. The syntheses, structures and nonlinear optical and related properties of salts with julolidinyl electron donor groups. Dyes and Pigm 2009;82:171–86.
[27] Ogawa J, Okada S, Glavcheva Z, Nakanishi H. Preparation, properties and structures of 1-methyl-4-{2-[4-(dimethylamino)phenyl]ethenyl} pyridinium crystals with various counter anions. J Cryst Growth 2008;310(4):836–42.
[28] Mutter L, Jazbinsek M, Zgonik M, Meier U, Bosshard C, Günter P. Photobleaching and optical properties of organic crystal 4-N,N-

dimethylamino-4′-N′-methyl stilbazolium tosylate. J Appl Phys 2003; 94(3):1356–61.

[29] Kurtz SK, Perry TT. A powder technique for the evaluation of nonlinear optical materials. J Appl Phys 1968;39:3798–813.

[30] Zyss J, Oudar JL. Relations between microscopic and macroscopic lowest-order optical nonlinearities of molecular-crystals with one-dimensional or two-dimensional units. Phys Rev A 1982;26:2028–48.

[31] Datta A, Pati SK. Dipolar interactions and hydrogen bonding in supramolecular aggregates: understanding cooperative phenomena for 1st hyperpolarizability. Chem Soc Rev 2006;35:1305–23.

[32] Bosshard C, Spreiter R, Günter P. Microscopic nonlinearities of two-component organic crystals. J Opt Soc Am B 2001;18:1620–6.

[33] Fujiwara M, Yanagi K, Maruyama M, Sugisaki M, Kuroyanagi K, Takahashi H, et al. Second order nonlinear optical properties of the single crystal of N-benzyl 2-methyl-4-nitroaniline: anomalous enhancement of the $d_{(333)}$ component and its possible origin. Jpn J Appl Phys 2006;45: 8676–85.

[34] Kwon OP, Jazbinsek M, Yun H, Seo JI, Kim EM, Lee YS, et al. Pyrrole-based hydrazone organic nonlinear optical crystals and their polymorphs. Cryst Growth Des 2008;8:4021–5.